CrossMark

RESEARCH ARTICLE

Performance Enhancements in Differential Ion Mobility Spectrometry-Mass Spectrometry (DMS-MS) by Using a Modified CaptiveSpray Source

Ri Wu,[1] Wei-Jing Wu,[1] Ze Wang,[1] Y.-L. Elaine Wong,[1] Y.-L. Winnie Hung,[1] H. T. Wong,[1] Xiangfeng Chen,[1,2] T.-W. Dominic Chan[1]

[1]Department of Chemistry, The Chinese University of Hong Kong, Hong Kong SAR, People's Republic of China
[2]Key Laboratory for Applied Technology of Sophisticated Analytical Instruments, Shandong Analysis and Test Centre, Qilu University of Technology (Shandong Academy of Sciences), Jinan, Shandong, People's Republic of China
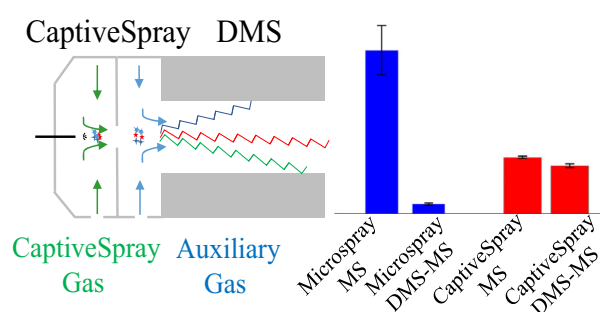
Abstract. Differential ion mobility spectrometry (DMS) spatially separates ions in the gas phase using the mobility differences of the ions under applied low and high electric fields. The use of DMS as an ion filter (or ion selector) prior to mass spectrometry analysis has been compromised by the limited ion transmission efficiency. This paper reports enhancement of the DMS-MS sensitivity and signal stability using a modified CaptiveSpray™ source. In terms of the ion sampling and transmission efficiency, the modified CaptiveSpray source swept ~ 89% of the ions generated by the tapered capillary through the DMS device (compared to ~ 10% with a conventional microspray source). The signal fluctuation improved from 11.7% (relative standard deviation, RSD) with microspray DMS-MS to 3.6% using CaptiveSpray-DMS-MS. Coupling of LC to DMS-MS via the modified CaptiveSpray source was simple and robust. Using DMS as a noise-filtering device, LC-DMS-MS performed better than conventional LC-MS for analyzing a BSA digest standard. Although LC-DMS-MS had a lower sequence coverage (55%), a higher Mascot score (283) was obtained compared to those of LC-MS (sequence coverage 65%; Mascot score 192) under the same elution conditions. The improvement in the confidence of the search result was attributed to the preferential elimination of noise ions.

Keywords: Differential ion mobility spectrometry, CaptiveSpray, Mass spectrometry, Ion filter

Introduction

Differential ion mobility spectrometry (DMS) was first introduced by Gorshkov et al. in 1982 [1]. This technique was later adopted by Buryakov and co-workers for detection of explosives and drugs and analysis of environmental samples [2, 3]. Charged species are orthogonally dispersed with respect to

the ion optical axis within the DMS gap by their mobility differences under alternating periods of high and low electric fields with opposite polarities. A DC potential difference (i.e., compensation voltage, CoV) is applied at the DMS electrodes to counter-balance the dispersion force induced on the ions by the asymmetric waveform. Upon scanning the CoV, ions with different dispersion properties will sequentially move through the DMS device. An ionogram is a plot of the ion signal intensity as a function of the CoV. DMS devices with planar [4, 5] and curved electrodes, e.g., cylindrical [6], semi-spherical, and spherical electrodes [7–9], have been developed and shown to display different analytical characteristics [10, 11]. DMS and field asymmetric waveform ion mobility

---

Correspondence to: Xiangfeng Chen; *e-mail:* xiangfchensdas@163.com, T.–W. Chan; *e-mail:* twdchan@cuhk.edu.hk

spectrometry (FAIMS) refer to devices with planar and curved electrodes, respectively [12]. Since the commercialization of DMS and FAIMS for use as post-ionization noise-filtering or ion separation devices in mass spectrometry, the number of published studies on these techniques has steadily increased over the past decades [12]. DMS and FAIMS have been used in combination with LC-MS and/or LC-MS/MS to improve signal-to-noise ratios (S/N) [13, 14], resulting in a higher Mascot score for protein identification [15–17]. Compared with low-field ion mobility spectrometry (IMS) techniques, such as drift-tube IMS [18], traveling-wave IMS [19], and trapped-ion IMS (TIMS) [20], DMS (or FAIMS) exhibits unique separation properties, but the factors governing the spatial dispersion of ions in DMS are not well understood [12]. There exist some correlations between the CoV of the ions and their collision cross-sections (CCS) for different members of a homologous series [21]. Both structural and conformational isomers can potentially be resolved in DMS (or FAIMS) [22]. However, the use of DMS has been limited by its analytical performance. Although the signal-to-noise ratios of the target ions typically improve with the use of a DMS device, the actual signal intensity decreases by almost an order of magnitude compared with the signal acquired without a DMS device [10, 11, 23]. In addition, the dispersion of ions by a DMS (or FAIMS) device is limited by the accessible asymmetric field. The use of gas modifiers has improved the situation by moving the peak positions to larger CoVs without significantly increasing the peak widths in the ionogram [24].

Different methods have been developed to boost the signal intensity and offset the ion loss in DMS (or FAIMS), including the use of a 1:1 He:N_2 mixture as a carrier gas [25], the addition of chemical modifiers [24], the use of an ion-confining electric field between the electrodes in DMS [10], and the use of asymmetric temperature settings for the outer and inner electrodes in cylindrical FAIMS [26]. An aerodynamic design of the ESI-FAIMS interface could enhance ion transmission and the sensitivity of a FAIMS device [10, 11, 27]. The use of a non-circular sampling aperture could increase the sampling region of a DMS device [28]. Coupling a slit interface to a multi-emitter electrospray ionization source could also enhance ion production and sampling [29]. Additional DC electrodes at the outlet of the planar electrodes could be used to create a DC barrier to confine the ion beam and reduce the lateral dispersion of the ions, creating a focusing field [30]. Using an inlet capillary with a large inner diameter or a rectangular aperture could also increase the ion transmission [6, 23]. An ion transfer capillary with a flared entrance could sample a greater number of ions from a DMS device than an unmodified standard capillary, and an ~ 5-fold increase in the signal sensitivity was achieved without changing the gas conductance [23].

Here, by coupling a modified CaptiveSpray source (Bruker, Billerica, MA, USA) [31, 32] to a typical DMS setup, we enhanced the resultant signal intensity and stability. Standard CaptiveSpray source has a high-voltage non-tapered capillary emitter enclosed in an airtight arrangement to allow for the vacuum of the mass spectrometer to pull ambient air into the source, directing a high percentage of sample ions into the mass spectrometer. In order to allow greater feasibility in choosing the flow rate of the carrier gas, a regulated gas flow was fed into the source to push the sample ions into the DMS device (see "Instrumentation" for details). Computational fluid dynamics (CFD) analyses were conducted, and different gas conditions were tested to determine the optimal gas flow dynamics at the CaptiveSpray-DMS interface. The transmission efficiency and stability of the CaptiveSpray-DMS and conventional microspray DMS devices were compared. An LC-DMS-MS analysis of a BSA trypsin digest was also conducted, and the results were compared with those from a corresponding LC-MS study using a CaptiveSpray interface.

Experimental Section

Chemicals

All materials were obtained commercially and used without further purification. Reserpine, β-casein, trypsin and LC-MS-grade methanol, acetonitrile, and water were purchased from Sigma-Aldrich (St. Louis, USA). The BSA digest MS standard (CAM-modified) was purchased from New England Bio Labs (Beijing, China). Reserpine was prepared at concentrations of 0.5 μM in a 1:1 methanol/water (v/v) mixture. The BSA digest MS standard was prepared at a concentration of 0.1 μM in water (v/v) for the LC-MS and LC-DMS-MS analyses. The digestion of β-casein was performed using a modified literature procedure [33]. Briefly, β-casein was digested by dissolving the protein in a 100 mM ammonium bicarbonate solution. Trypsin was dissolved in 50 mM acetic acid and mixed with the protein solution at a trypsin to protein ratio of 1:30. The mixtures were incubated overnight (14 h) at 37 °C. The final solution was kept at – 20 °C prior to analysis.

DMS Setup

Figure 1 shows the homemade DMS device used in the present study. The device contained a hollowed rectangular PEEK (Gher, HK) housing in which two rectangular stainless-steel blocks (20 mm height × 80 mm length) were mounted on opposite interior sides of the housing to serve as the DMS electrodes. A series of these electrodes were machined with different thicknesses to obtain a DMS device with three different channel heights, i.e., 0.6, 1.4, and 2.0 mm. One end of the PEEK housing was fitted with an end plate, which was mounted against the dielectric capillary of the FTICR-MS instrument in an airtight fashion. The other end of the PEEK housing was attached to a circular PEEK chamber. The PEEK chamber had a gas inlet on the side so that an auxiliary gas (a regulated nitrogen gas flow in the range of 0–5000 mL/min) can be orthogonally inserted, i.e., with respect to the sampling orifice and the DMS channel, and dispersed into the co-axial gas flow. The auxiliary gas flow was controlled using a FC-2901MEP mass flow controller (2900 series, Tylan General Inc., USA) and monitored by a flow meter (Key Instruments,
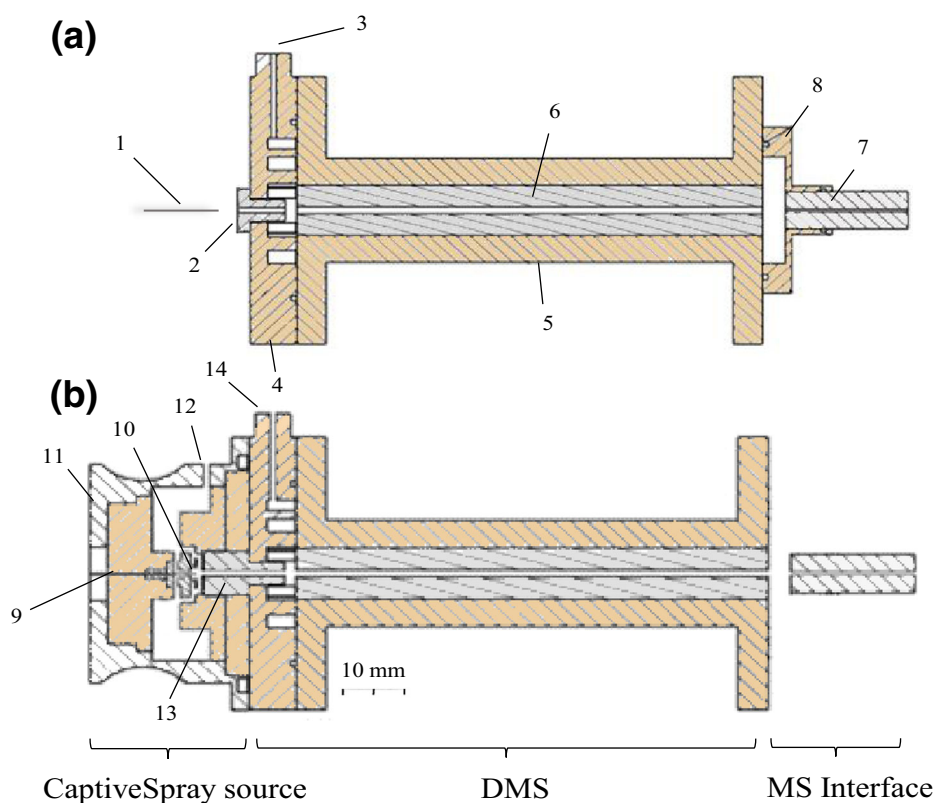
Figure 1. (a) A schematic diagram of the microspray DMS setup. 1. Microspray capillary tip; 2. DMS inlet; 3. Auxiliary gas inlet; 4. Circular PEEK chamber; 5. PEEK housing; 6. DMS planar electrodes; 7. FTICR-MS dielectric capillary inlet. 8. Airtight end plate. (b) A schematic diagram of the CaptiveSpray-DMS setup. 9. Sample inlet; 10. Tapered fused silica capillary tip; 11. Sealed CaptiveSpray chamber; 12. CaptiveSpray gas inlet; 13. DMS inlet; 14. Auxiliary gas inlet

UK). The center of the front plate of the PEEK chamber had an electrically ground stainless-steel nut with a 1.4-mm (or 2.0 mm) (i.d.) orifice for ion sampling from the external ionization source. The details of the electronics of DMS are shown in the Supporting Information [34].

Instrumentation

All experiments were performed on a Bruker SolariX FTICR-MS equipped with a 9.4 T actively shielded refrigerated magnet. The analyte solution was delivered using a LEGATO 110 syringe pump (Kd Scientific Inc., USA) at a flow rate of 30 μL/h via a silica capillary (i.d. 50 μm). The capillary was mounted on a three-axis stage and positioned ~ 1.5 mm away from the entrance orifice of the DMS device. A microspray was generated at the tip of the capillary by floating the analyte solution at + 3.0 kV. For the CaptiveSpray-DMS experiments, the standard CaptiveSpray source was directly mounted on the circular PEEK chamber. The CaptiveSpray source was maintained at a voltage of 1.3 kV. Instead of pulling air into the CaptiveSpray source by the suction of the mass spectrometry inlet, a regulated nitrogen gas flow (99.99%, AP, China) was fed into the source by using a FC-2901MEP mass flow controller (2900 series, Tylan General Inc., USA) and flow meter (Key Instruments). The nitrogen flow facilitated the collection of the sprayed ions towards the inlet of the DMS chamber. In order

to allow greater feasibility in the use of CaptiveSpray and auxiliary gas flows, the end plate that holds the DMS chamber against the dielectric capillary of the FTICR-MS was removed. In this way, the gas flow across the DMS chamber was solely controlled by the sum of the CaptiveSpray and the auxiliary gas flows. The vacuum conditions of the inlet region of the FTICR-MS would not be affected even if the total gas flow across the DMS chamber exceeds the gas dragging rate of 1300 mL/min at the dielectric capillary. Analyte solution was delivered to the CaptiveSpray source using a LEGATO 110 syringe pump (Kd Scientific, USA) at a flow rate of 30 μL/h. A homemade LabVIEW (version 2013, 32 bit, National Instruments, U.S.) program was written to control the compensation voltage (CoV) via a GPIB-USB-HS with a user-friendly GUI. For recording the DMS ionogram, the FTMS pulse sequence was modified to include a TTL pulse to trigger the stepping of the CoV after each mass spectral acquisition. Ionograms of selected ion were processed using Origin Pro 8 (OriginLab, Northampton, MA).

For the LC-MS and LC-DMS-MS experiments, the protein digest solutions were chromatographically separated using an Acclaim™ PepMap™ 100 C18 LC Column (75 μm × 150 mm × 3 μm, 100 Å). The output was coupled directly to the FTICR-MS via the CaptiveSpray source. The details of the DMS-MS and LC-MS experimental conditions are shown in the Supporting Information.

Results and Discussion

In the present CaptiveSpray-DMS arrangement, the CaptiveSpray gas flow creates an air funnel that sweeps the spray from the capillary tip and pushes the ions towards the DMS chamber. The auxiliary gas flow is used to ensure that the overall carrier gas flow in the DMS chamber can be controlled and is independent of the gas flow conditions for optimum nebulization and focusing of the sprayed ions.

Effect of the Gas Flow Conditions on the Signal Intensity

The impact of the CaptiveSpray and auxiliary gas flows on the performance of the DMS device was experimentally investigated. In this experiment, the CaptiveSpray gas flow rate was systematically varied from 300 to 900 mL/min in step sizes of 300 mL/min. For each CaptiveSpray flow rate, a series of reserpine ion ionograms were systematically obtained using different auxiliary gas flows. Table S1 summarizes the intensities, CoV maximum values, and full-width-half-maximum (FWHM) values of the reserpine signal profiles in the ionograms obtained under different gas flow conditions. The ionograms are shown in Figure S1 (see Supporting Information). To eliminate the impact of the signal intensity on the FWHM of the ionogram, different ion accumulation times were used to maintain the overall signal intensities in the range of 2E + 8 to 2E + 9 (arbitrary scale). A correlation between the CaptiveSpray gas flow and the ion intensities was deduced based on the ion accumulation times and the signal intensities. For acquisitions using the same overall carrier gas flow rate (i.e., 0.5 CaptiveSpray flow rate + auxiliary gas flow rate), increasing the CaptiveSpray gas flow resulted in reserpine ion signals with higher intensities. This correlation was tentatively attributed to the sweeping rate of the sample solution from the spray tip increasing due to the higher CaptiveSpray gas flow. For a specific CaptiveSpray flow rate, the reserpine ion signal could be improved by using a higher auxiliary gas flow. This is consistent with the auxiliary gas flow reducing gas expansion at the exit of the CaptiveSpray chamber.

The effect of the carrier gas (auxiliary gas) flow on the reserpine signal responses using the conventional microspray DMS setup is also included in Table S1 for comparison. The reserpine ion signal was only registered in a narrow range of carrier gas flow rates. A very weak reserpine signal was observed in the absence of a carrier gas flow. The signal increased with the carrier gas flow rate and reached a maximum at ~ 200 mL/min, but then, the signal rapidly declined at higher carrier gas flow rates. No reserpine signal was registered at carrier gas flow rates higher than 600 mL/min. In a conventional microspray DMS arrangement, the flow direction of the carrier gas depends on the gas drag rate of the mass spectrometer inlet and the loading of the carrier gas. With zero or a low carrier gas flow, the sprayed ions and surrounding air molecules will be sucked into the DMS compartment and moved by the carrier gas towards the mass spectrometer inlet. At a high carrier gas loading (i.e., > 200 mL), the carrier gas should flow in both directions. A portion of the loaded gas should move towards the mass spectrometer inlet, while another portion should flow towards the sprayer. At a moderate carrier gas flow, the outward flow may assist in the desolvation of the sprayed droplets and improve the reserpine signal. As the carrier gas loading increases, the counter flow of gas may blow the sprayed droplets away and cause a reduction in the reserpine signal. In contrast to the conventional microspray DMS arrangement, CaptiveSpray-DMS has an airtight arrangement at the sprayer compartment. The CaptiveSpray gas and the entrained sample ions can flow only in the direction of the mass spectrometer inlet. This accounts for the superior ion collection and transmission efficiency of CaptiveSpray-DMS devices. A strong reserpine signal was observed throughout the range of gas flow rates tested in the present study (i.e., 300 to 1800 mL/min).

Effect of the Gas Flow Conditions on the Resolving Power

The analyte peak width in an ionogram indicates the resolving power. The resolving power of DMS has previously been associated with many experimental parameters, such as the carrier gas composition [35], ion residual time in the DMS channel [4], and DMS device geometry [17]. The use of high helium content carrier gas results in peaks with a narrower FWHM [35]. Additional polar gas modifiers can shift the peak position of an analyte and increase the resolving power based on the classical equation, R = CoVmax/FWHM [17, 36]. For a particular carrier gas flow rate, narrowing the channel height increases the carrier gas flow velocity and reduces the residence time of the ions in the DMS channel. Thus, the ion beam has less time to laterally diffuse, and a smaller CoV range is required to deflect the ion beam away from the sampling cone of the mass spectrometer inlet. Table S1 summarizes the variations in the CoV maximum and FWHM values of the protonated reserpine species in the ionogram obtained under different CaptiveSpray and auxiliary gas flow combinations. Regardless of the gas flow conditions, the CoV maximum value of reserpine was fairly stable. The reserpine peak widths in the ionograms displayed different trends. Both the CaptiveSpray and auxiliary gas flows affected the FWHM values of the reserpine ionograms. For a particular CaptiveSpray gas flow, the FWHM well correlated with the auxiliary gas flow. A higher auxiliary gas flow led to a broader reserpine ionogram. However, the influence of the CaptiveSpray gas flow was more profound. Increasing the CaptiveSpray gas flow rate from 300 to 600 mL/min increased the FWHM of the reserpine ionogram by 40–60%. A further increase in the CaptiveSpray gas flow rate to 900 mL/min resulted in a smaller % increase in the FWHM (7–15%).

CFD Simulation of the Gas Flow Dynamics

To investigate the effect of the CaptiveSpray and auxiliary gas flows on the overall carrier gas movement in the DMS
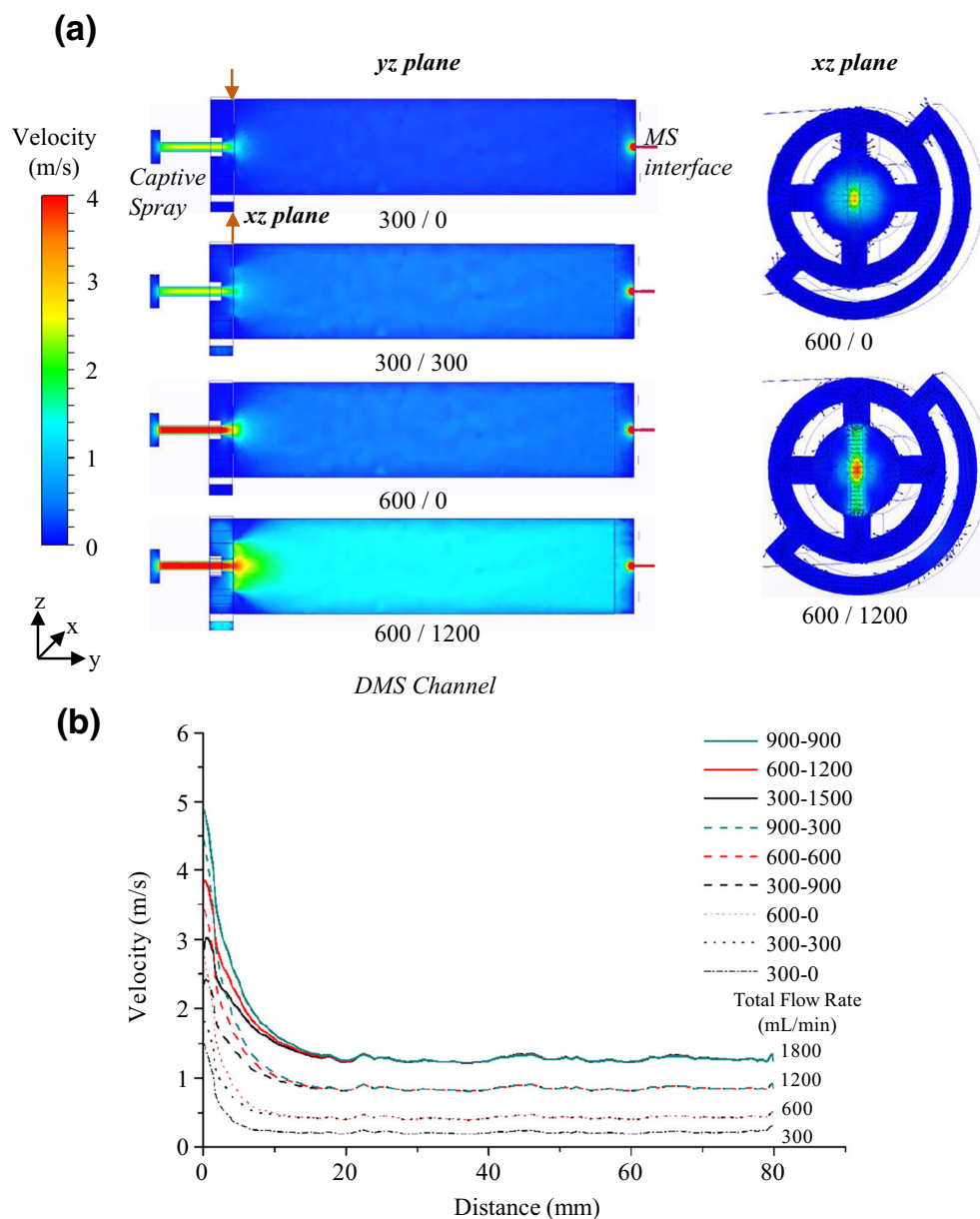
Figure 2. CFD simulation results for CaptiveSpray-DMS. (**a**) Yz-plane and xz-plane images from a 3D CFD simulation of the gas flow in a CaptiveSpray-DMS system using different CaptiveSpray and auxiliary gas flow conditions. (**b**) Plots of the axial velocity of the gas molecules along the DMS device using different CaptiveSpray and auxiliary gas flow conditions

chamber, a CFD simulation study was conducted. Figure 2 shows the CFD simulation results for the CaptiveSpray-DMS. Figure 2A shows the yz-plane images from the 3D CFD simulation of the gas flow in the CaptiveSpray-DMS system under different CaptiveSpray/auxiliary gas flow conditions. As shown in Figure 2A, the gas flow velocity was the highest at the exit channel of the CaptiveSpray chamber, which is where the gas conductance was the smallest. In the absence of an auxiliary gas flow, the CaptiveSpray gas expands at the exit orifice and rapidly slows down in the front part of the DMS channel. The xz-plane images of the DMS entrance at the higher CaptiveSpray flow rate (i.e., 600 mL/min) are shown in the right. Presumably due to the rectangular nature of the cross-section of the DMS channel, the gas expands to fill the

channel along the x-direction and continuously expands along the y-direction.

Based on the gas entrainment effect, the reserpine ions were assumed to have a velocity distribution similar to that of the carrier gas molecules. To obtain more information, Figure 2B shows the axial velocity distribution of the carrier gas molecules (or reserpine ions) as a function of the position along the DMS channel. The simulation data show that the initial axial velocity of the carrier gas molecules (at the entrance of the DMS channel) positively correlates with the CaptiveSpray gas flow, and the final axial velocity of the carrier gas molecules (at the exit of the DMS channel) depends solely on the sum of the CaptiveSpray and auxiliary gas flows. Owing to the small orifice separating the CaptiveSpray chamber and the DMS

device, the initial axial velocity of the carrier gas molecules is significantly higher than the final axial velocity. Due to collisional cooling, the axial velocity of the gas molecules rapidly decreased in the entrance region of the DMS channel. Within 10 to 20 mm, the axial velocity of the carrier gas molecules decreased to a steady state value governed by the sum of the CaptiveSpray and auxiliary gas flows.

Owing to the static boundary conditions on the electrode surfaces, the axial velocity of the gas flows has a quasi-parabolic profile across the DMS channel height [37]. The gas velocity dispersion (Δv) among the carrier gas molecules should range from zero to the maximum axial velocity, which in turn should be governed by the CaptiveSpray and auxiliary gas flow conditions. In the comparative study shown in Table S1, the FWHM of the reserpine ion peak became wider due to the additive effects of Δv in the initial state and steady state regions within the DMS channel. To obtain a good resolving power, the CaptiveSpray and auxiliary gas flows should be minimized with an acceptable ion transmission efficiency.

Effect of the Channel Height and Asymmetric Field Strength

In this study, three different channel heights were studied using a fixed gas flow condition, i.e., a CaptiveSpray gas flow of 300 mL/min and an auxiliary gas flow of 600 mL/min. For each channel height, the effect of the asymmetric field (Vp-p or Td) was systematically investigated. The results are summarized in Table S2. The ionograms are shown in Figure S2 (see Supporting Information). A noticeable advantage of using the CaptiveSpray source in the DMS-MS experiment was the minimal influence of the channel height and the asymmetric field strength on the intensity of the protonated reserpine signals. This was illustrated by the fact that the reserpine signal was observed with an acceptable intensity in a dispersion field of 207 Td by optimizing the CaptiveSpray and auxiliary gas flows using a

DMS device with a 0.6-mm channel height (data not shown). In conventional microspray DMS-MS, the analyte ion signal (or the ion transmission efficiency) decreases sharply with the decreasing channel height and/or with the use of a higher asymmetric field strength (data not shown) [38]. Apart from the ion transmission efficiency, the CaptiveSpray-DMS exhibited performance behavior similar to that of conventional microspray DMS. Increasing the channel height shifted the CoV maximum away from zero and broadened the FWHM of the reserpine ion peak in the ionogram. At a particular channel height, increasing the asymmetric field strength shifted the CoV maximum away from zero with no significant impact on the FWHM of the ion peak in the ionogram. The use of narrower DMS channels and high asymmetric fields can maximize the resolving power of CaptiveSpray-DMS-MS. For the protonated reserpine species, a resolving power 4.5 can be obtained by using DMS with a channel height of 1.4 mm without using any gas modifiers.

Ion Transmission Efficiency and Stability

To obtain a good resolving power and reasonable ion transmission efficiency, the CaptiveSpray and auxiliary gas flows were experimentally re-optimized. A CaptiveSpray gas flow rate of 350 mL/min and an auxiliary gas flow rate of 300 mL/min resulted in the optimum performance. To assess the performance enhancement obtained using the CaptiveSpray source, additional experiments were conducted to compare the reserpine ion signals using different source arrangements. Figure 3A shows the signal intensities of the reserpine ions obtained using microspray MS with and without DMS and CaptiveSpray MS with and without DMS. Using a conventional microspray source, a significant drop in the intensity of the protonated reserpine signal was observed by simply inserting the DMS device between the microspray source and the mass spectrometry inlet. The ion collection and transmission efficiencies both decreased by ~ 90%. Using the CaptiveSpray source, only a
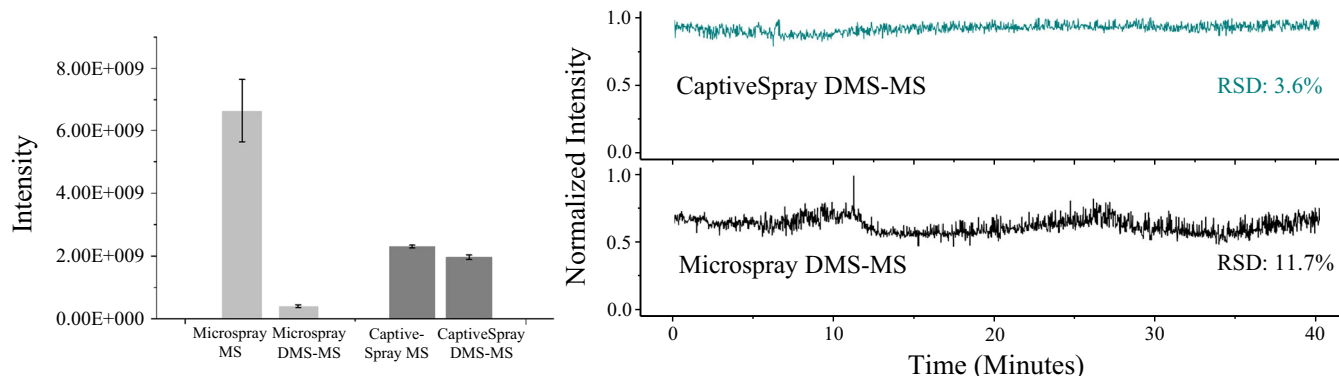

Figure 3. (a) Signal intensity of the reserpine ion signal obtained from conventional microspray MS with and without DMS; CaptiveSpray MS with and without DMS. (b) Signal intensity and stability of the reserpine ion signal using CaptiveSpray-DMS and conventional microspray DMS setup. Conditions, channel height is 2.0 mm; dispersion field is 100 Td. CaptiveSpray-DMS conditions, CaptiveSpray gas flow rate of 350 mL/min, auxiliary gas flow rate of 300 mL/min; ion accumulation time of 0.5 s; Conventional microspray DMS conditions, auxiliary gas flow rate of 300 mL/min; ion accumulation time of 0.5 s

small decrease in the intensity of the protonated reserpine signal was observed under otherwise identical experimental conditions. The ion collection and transmission efficiencies decreased by ~ 11%. Figure 3B shows the plots of the normalized reserpine signal as a function of time for a period of 40 min using CaptiveSpray-DMS-MS (top) and microspray DMS-MS (bottom). In addition to the higher average signal intensity (1.96E9 versus 3.99E8), the stability of the CaptiveSpray-DMS-MS signal (%RSD = 3.6) was significantly better than that obtained by microspray DMS-MS (%RSD = 11.7).

Bottom-up Protein Identification

The CaptiveSpray source was developed as a robust ion source to couple liquid chromatographic systems with a mass spectrometer. The source works well with a wide variety of solvent compositions and solution flow rates and offers a wider dynamic range than conventional nanospray sources. To show that the advantages of CaptiveSpray source in coupling with LC-MS are retained in LC-DMS-MS, a protein digest was analyzed using both LC-DMS-MS and LC-MS with CaptiveSpray source.

For bottom-up protein identification using LC-DMS-MS peptide mapping, DMS operating at a static CoV value was employed. In this case, DMS served as a noise-filtering device. To achieve a high transmission of tryptic digest fragment ions and reasonable truncation of unwanted ion noise, a DMS device with a channel height of 2.0 mm was used. To obtain sensible settings for the DMS device, low- (50 Td), medium- (75 Td), and high- (100 Td) field ionograms of the tryptic digest of β-casein were obtained using a direct infusion method with the CaptiveSpray source. The ionograms are shown in Figure S3 (see Supporting Information). As expected, in the low-field ionogram (50 Td), the CoV maxima for almost all the digest components were displaced to − 0.5 V. No separation of individual components was observed in the DMS dimensional space. In the medium-field ionogram (75 Td), the digest components were charge separated in the DMS dimensional space. The CoV maxima for the singly, doubly, and triply charged tryptic digest ions were − 0.9, − 1.5, and − 2.2 V, respectively. In the high-field ionogram, the CoV positions of different tryptic digest ions depended on the charge states and nature of the ions. The CoV maxima for different tryptic digest ions were spread across a CoV range from − 2 to − 5.5 V.

For the comparative study, DMS with a channel height of 2.0 mm and a medium asymmetric field of 75 Td were selected. These arrangements would lead to good overlap between ions with the same charge states. Three static CoVs (− 0.9 V, − 1.5 V, and − 2.2 V) were used in the LC-DMS-MS for optimal transmission of singly, doubly, or triply charged ions through the DMS device. Due to the hydrophobic nature of β-casein, a significant number of the tryptic digest fragments were a result of cleavage at unexpected sites [39]. This will severely affect the reliability of the Mascot search. Therefore, the comparative study was conducted using a BSA tryptic digest.

A bottom-up protein identification using a Mascot search of tryptic digest fragments obtained by LC-MS (or LC-DMS-MS) relies on the quality of the submitted peak list. For the same data set, the submission of a peak list with different noise cutoffs can result to different numbers of submitted peaks and different Mascot scores. A systematic study using a 0 to 10% signal cutoff and extracting 1 to 50 of the most abundant peaks from the LC-MS data showed that a 2.5% cutoff with the extraction of the 10 most abundant peaks in each chromatographic peak resulted in the highest Mascot score (i.e., 192) with sequence coverage at the 65% level. A higher or lower signal cutoff level resulted in a lower Mascot score. Therefore, the criteria of a 2.5% signal cutoff and an extraction of the 10 most abundant peaks were used to treat the LC-MS and LC-DMS-MS datasets. Table 1 and Figure S-4 (Supporting Information) show a summary of the sequence coverages and Mascot scores for the LC-MS and LC-DMS-MS data using a 2.5% signal cutoff. The use of − 1.5 and − 2.2 V CoVs produced very good search results with Mascot scores of 283 and 305, respectively. The sequence coverages at these CoVs (55 and 49%) were slightly lower than those obtained from LC-MS (65%). This result was consistent with the general expectation that the tryptic digest of BSA produced peptide fragments with lengths appropriate for the formation of doubly protonated and triply protonated species and that most of the "noise" peaks generated under typical spray ionization conditions were singly charged. A moderate CoV would filter out a large number of noise peaks and allow most of the BSA digest fragment ions to pass. It is perhaps important to note that the slight reduction of the sequence coverage in LC-DMS-MS is primarily caused by the use of a static CoV. Stepping of CoV within a LC run (internal stepping) or in-between LC runs (external stepping) has shown to give a greater sequence coverage than LC-MS [12, 40, 41].

Conclusions

A CaptiveSpray source was successfully incorporated into a DMS-MS system. Instead of sucking the spray ions into the DMS channel for separation, the gas flow conditions of the modified CaptiveSpray source swept and pushed the spray ions into the DMS channel. The addition of an auxiliary gas at the exit of the CaptiveSpray housing alleviated the gas expansion and led to a streamline flow of the carrier gas through the DMS

Table 1. A summary of the sequence coverage and Mascot scores obtained from the LC-CaptiveSpray-MS and LC-CaptiveSpray-DMS-MS chromatograms of 200 fmol BSA tryptic digest at three different CoVs (− 0.9, − 1.5, and − 2.2 V) using a dispersion field of 75 Td (channel height, 2.0 mm; ion accumulation time, 0.5 s)

	Protein sequence coverage	Mascot search score
LC-MS	65%	192
LC-DMS-MS (− 0.9 V)	51%	210
LC-DMS-MS (− 1.5 V)	55%	283
LC-DMS-MS (− 2.2 V)	49%	305

channel. By removing the end plate of the DMS device, a larger range of CaptiveSpray and auxiliary gas flow rates could be used without affecting the inlet pressure conditions of the mass spectrometer. The FWHM of the reserpine ionogram was optimized by modulating the absolute and relative flows of the CaptiveSpray and auxiliary gases without significantly compromising the ion transmission efficiency. A high ion transmission efficiency (~ 89%) across the DMS device to the MS was achieved. Similar to CaptiveSpray LC-MS, CaptiveSpray LC-DMS-MS displayed a stable spray under the whole gradient elution range. Pre-setting DMS to a static CoV of − 1.5 V (or 2.2 V) could generate LC-DMS-MS data that retained most of the tryptic digest fragments and eliminated most of the noise ions. At the 2.5% noise cutoff, LC-DMS-MS produced a higher Mascot score (305) than the corresponding LC-MS data (192).

Acknowledgements

Funding Information

References

1. Gorshkov, M. P.: SU 966,583 G01N27/62 (1982)
2. Buryakov, I.A., Krylov, E.V., Makas, A.L., Nazarov, E.G., Pervukhin, V.V., Rasulev, U.K.: Separation of ions according to mobility in a strong AC electric field. Sov. Tech. Phys. Lett. **17**, 446–447 (1991)
3. Buryakov, I.A., Krylov, E.V., Nazarov, E.G., Rasulev, U.K.: A new method of separation of multi-atomic ions by mobility at atmospheric pressure using a high-frequency amplitude-asymmetric strong electric field. Int. J. Mass Spectrom. Ion Process. **128**, 143–148 (1993)
4. Schneider, B.B., Covey, T.R., Coy, S.L., Krylov, E.V., Nazarov, E.G.: Planar differential mobility spectrometer as a pre-filter for atmospheric pressure ionization mass spectrometry. Int. J. Mas. Spectrom. **298**, 45–54 (2010)
5. Shvartsburg, A.A., Li, F., Tang, K., Smith, R.D.: High-resolution FAIMS using new planar geometry analyzers. Anal. Chem. **78**, 3706–3714 (2006)
6. Swearingen, K.E., Winget, J.M., Hoopmann, M.R., Kusebauch, U., Moritz, R.L.: Decreased gap width in a cylindrical FAIMS device improves protein discovery. Anal. Chem. **87**, 12230–12237 (2015)
7. Guevremont, R., Barnett, D.A., Purves, R.W., Vandermey, J.: Analysis of a tryptic digest of pig hemoglobin using ESI-FAIMS-MS. Anal. Chem. **72**, 4577–4584 (2000)
8. Purves, R.W., Guevremont, R.: Electrospray ionization high-field asymmetric waveform ion mobility spectrometry–mass spectrometry. Anal. Chem. **71**, 2346–2357 (1999)
9. Prieto, S., Yost, R.: Spherical FAIM. Comparison of curved electrode geometries. Int. J. Ion Mobil. Spectrom. **14**(2), 61–69 (2011)
10. Prasad, S., Belford, M.W., Dunyach, J.J., Purves, R.W.: On an aerodynamic mechanism to enhance ion transmission and sensitivity of FAIMS for nano-electrospray ionization-mass spectrometry. J. Am. Soc. Mass Spectrom. **25**, 2143–2153 (2014)
11. Schneider, B.B., Londry, F., Nazarov, E.G., Kang, Y., Covey, T.R.: Maximizing ion transmission in differential mobility spectrometry. J. Am. Soc. Mass Spectrom. **25**, 2151–2159 (2017)
12. Cooper, H.J.: To what extent is FAIMS beneficial in the analysis of proteins? J. Am. Soc. Mass Spectrom. **27**, 566–577 (2016)
13. Arthur, K.L., Turner, M.A., Brailsford, A.D., Kicman, A.T., Cowan, D.A., Reynolds, J.C., Creaser, C.S.: Rapid analysis of anabolic steroid metabolites in urine by combining field asymmetric waveform ion mobility spectrometry with liquid chromatography and mass spectrometry. Anal. Chem. **89**, 7431–7437 (2017)
14. Fu, Y., Xia, Y.Q., Flarakos, J., Tse, F.L., Miller, J.D., Jones, E.B., Li, W.: Differential mobility spectrometry coupled with multiple ion monitoring in regulated LC-MS/MS bioanalysis of a therapeutic cyclic peptide in human plasma. Anal. Chem. **88**, 3655–3661 (2016)
15. Brown, L.J., Toutoungi, D.E., Devenport, N.A., Reynolds, J.C., Kaur-Atwal, G., Boyle, P., Creaser, C.S.: Miniaturized ultra high field asymmetric waveform ion mobility spectrometry combined with mass spectrometry for peptide analysis. Anal. Chem. **82**, 9827–9834 (2010)
16. Bridon, G., Bonneil, E., Muratore-Schroeder, T., Caron-Lizotte, O., Thibault, P.: Improvement of phosphoproteome analyses using faims and decision tree fragmentation. Application to the insulin signalling pathway in drosophila melanogaster s2 cells. J. Proteome Res. **11**, 927–940 (2011)
17. Bonneil, E., Pfammatter, S., Thibault, P.: Enhancement of mass spectrometry performance for proteomic analyses using high-field asymmetric waveform ion mobility spectrometry (FAIMS). J. Mass Spectrom. **50**, 1181–1195 (2015)
18. Dwivedi, P., Bendiak, B., Clowers, B.H., Hill, H.H.: Rapid resolution of carbohydrate isomers by electrospray ionization ambient pressure ion mobility spectrometry-time-of-flight mass spectrometry (ESI-APIMS-TOFMS). J. Am. Soc. Mass Spectrom. **18**, 1163–1175 (2007)
19. Giles, K., Pringle, S.D., Worthington, K.R., Little, D., Wildgoose, J.L., Bateman, R.H.: Applications of a travelling wave-based radio-frequency-only stacked ring ion guide. Rapid Commun. Mass Spectrom. **18**, 2401–2414 (2004)
20. Pu, Y., Ridgeway, M.E., Glaskin, R.S., Park, M.A., Costello, C.E., Lin, C.: Separation and identification of isomeric glycans by selected accumulation-trapped ion mobility spectrometry-electron activated dissociation tandem mass spectrometry. Anal. Chem. **88**, 3440–3443 (2016)
21. Auerbach, D., Aspenleiter, J., Volmer, D.A.: Description of gas-phase ion/neutral interactions in differential ion mobility spectrometry: COV prediction using calibration runs. J. Am. Soc. Mass Spectrom. **25**, 1610–1621 (2014)
22. Schneider, B.B., Nazarov, E.G., Londry, F., Vouros, P., Covey, T.R.: Differential mobility spectrometry/mass spectrometry history, theory, design optimization, simulations, and applications. Mass Spectrom. Rev. **35**, 687–737 (2016)
23. Campbell, M.T., Glish, G.L.: Increased ion transmission for differential ion mobility combined with mass spectrometry by implementation of a flared inlet capillary. J. Am. Soc. Mass Spectrom. **28**, 119–124 (2017)
24. Schneider, B.B., Covey, T.R., Coy, S.L., Krylov, E.V., Nazarov, E.G.: Chemical effects in the separation process of a differential mobility/mass spectrometer system. Anal. Chem. **82**, 1867–1880 (2010)
25. Barnett, D.A., Ells, B., Guevremont, R., Purves, R.W.: Application of ESI-FAIMS-MS to the analysis of tryptic peptides. J. Am. Soc. Mass Spectrom. **13**, 1282–1291 (2002)
26. Barnett, D.A., Belford, M., Dunyach, J.J., Purves, R.W.: Characterization of a temperature-controlled FAIMS system. J. Am. Soc. Mass Spectrom. **18**, 1653–1663 (2007)
27. Purves, R.W., Prasad, S., Belford, M., Vandenberg, A., Dunyach, J.J.: Optimization of a new aerodynamic cylindrical FAIMS device for small molecule analysis. J. Am. Soc. Mass Spectrom. **28**, 525–538 (2017)
28. Tang, K., Shvartsburg, A. A., Smith, R. D.: Interface and process for enhanced transmission of non-circular ion beams between stages at unequal pressure. U.S. Patent 7,339,166, (2008)
29. Mabrouki, R., Kelly, R.T., Prior, D.C., Shvartsburg, A.A., Tang, K., Smith, R.D.: Improving FAIMS sensitivity using a planar geometry with slit interface. J. Am. Soc. Mass Spectrom. **20**, 1768–1774 (2009)
30. Belford, M. W., Kovtoun, V. V.: Flat plate FAIMS with lateral ion focusing. U.S. Patent 7,851,745, (2010)
31. Nugent, K., Zhu, Y., Kent, P., Phinney, B., Alvarado, R.: Captive spray: a new ionization technique to maximizing speed, sensitivity, resolution and robustness for LCMS protein biomarker quantitation. Proceedings of the

57th ASMS Conference on Mass Spectrometry and Allied Topics, ASMS, Philadelphia, PA (2009)

32. Ramanathan, R., Raghavan, N., Comezoglu, S.N., Humphreys, W.G.: A low flow ionization technique to integrate quantitative and qualitative small molecule bioanalysis. Int. J. Mass Spectrom. **301**, 127–135 (2011)

33. Yeung, H.S., Chen, X., Li, W., Wang, Z., Wong, Y.E., Chan, T.W.D.: Development of miniaturized sorbent membrane funnel-based spray platform for biological analysis. Anal. Chem. **87**, 3149–3153 (2015)

34. Canterbury, J.D., Gladden, J., Buck, L., Olund, R., MacCoss, M.J.: A high voltage asymmetric waveform generator for FAIMS. J. Am. Soc. Mass Spectrom. **21**, 1118–1121 (2010)

35. Shvartsburg, A.A., Prior, D.C., Tang, K., Smith, R.D.: High-resolution differential ion mobility separations using planar analyzers at elevated dispersion field. Anal. Chem. **82**, 7649–7655 (2010)

36. Purves, R.W., Ozog, A.R., Ambrose, S.J., Prasad, S., Belford, M., Dunyach, J.J.: Using gas modifiers to significantly improve sensitivity and selectivity in a cylindrical FAIMS device. J. Am. Soc. Mass Spectrom. **25**, 1274–1284 (2014)

37. Shvartsburg, A.A., Smith, R.D.: Scaling of the resolving power and sensitivity for planar FAIMS and mobility-based discrimination in flow- and field-driven analyzers. J. Am. Soc. Mass Spectrom. **18**, 1672–1681 (2007)

38. Blagojevic, V., Chramow, A., Schneider, B.B., Covey, T.R., Bohme, D.K.: Differential mobility spectrometry of isomeric protonated dipeptides: modifier and field effects on ion mobility and stability. Anal. Chem. **83**, 3470–3476 (2011)

39. Tan, P.S., Van Kessel, T.A., Van de Veerdonk, F.L., Zuurendonk, P.F., Bruins, A.P., Konings, W.N.: Degradation and debittering of a tryptic digest from beta-casein by aminopeptidase N from Lactococcus lactis subsp. cremoris Wg2. Appl. Environ. Microbiol. **59**, 1430–1436 (1993)

40. Creese, A.J., Shimwell, N.J., Larkins, K.P., Heath, J.K., Cooper, H.J.: Probing the complementarity of FAIMS and strong cation exchange chromatography in shotgun proteomics. J. Am. Soc. Mass Spectrom. **24**(3), 431–443 (2013)

41. Canterbury, J.D., Yi, X., Hoopmann, M.R., MacCoss, M.J.: Assessing the dynamic range and peak capacity of nanoflow LC-FAIMS-MS on an ion trap mass spectrometer for proteomics. Anal. Chem. **80**(18), 6888–6897 (2008)